Supporting Information

Tables S1-S4 and Figures S1-S8

Tick and host derived compounds modulate the biochemical properties of the cement complex substance

Margarita Villar[1,2§], Iván Pacheco[1§], Octavio Merino[3§], Marinela Contreras[1§], Lourdes Mateos-Hernández[1,4], Eduardo Prado[5], Dina Karen Barros-Picanço[1], José Francisco Lima-Barbero[1,6], Sara Artigas-Jerónimo[1], Pilar Alberdi[1], Isabel G. Fernández de Mera[1], Agustín Estrada-Peña[7], Alejandro Cabezas-Cruz[4], José de la Fuente[1,8]

[1]SaBio, Instituto de Investigación en Recursos Cinegéticos (IREC-CSIC-UCLM-JCCM), Ronda de Toledo s/n, 13005 Ciudad Real, Spain.

[2]Biochemistry Section, Faculty of Science and Chemical Technologies, and Regional Centre for Biomedical Research (CRIB), University of Castilla-La Mancha, 13071, Ciudad Real, Spain.

[3]Facultad de Medicina Veterinaria y Zootecnia, Universidad Autónoma de Tamaulipas, Km 5, Carretera Victoria–Mante, CP 87000 Ciudad Victoria, Tamaulipas, Mexico.

[4]UMR BIPAR, INRA, ANSES, Ecole Nationale Vétérinaire d'Alfort, Université Paris-Est, Maisons-Alfort, 94700, France.

[5]Department of Applied Physics, Faculty of Chemical Sciences and Technologies, Universidad de Castilla-La Mancha, Avda. Camilo José Cela 10, 13071 Ciudad Real, Spain.

[6]Sabiotec, Camino de Moledores s/n. 13003, 13071 Ciudad Real, Spain.

[7]Facultad de Veterinaria, Universidad de Zaragoza, 50013 Zaragoza, Spain.

[8]Department of Veterinary Pathobiology, Center for Veterinary Health Sciences, Oklahoma State University, Stillwater, OK 74078, USA.

[§]Equal contribution.

Email: jose_delafuente@yahoo.com / josedejesus.fuente@uclm.es

Table S1. *R. microplus* tick-derived proteins identified in the cementome.

Protein ID, name and (criteria for selection)	**Representation profile category**	**Biological Process**
V5HZA1 Histone H2A (a, c)	SG: Feeding & oogenesis CE: Feeding & oogenesis	Protein heterodimerization
V5HJX3 Histone H2A (b, c)	CE: Feeding & oogenesis	Protein heterodimerization
L7LVH9 Histone H3 (a, c)	SG: Feeding & oogenesis CE: Detachment	Protein heterodimerization
Q4PM69¶* Histone H4 (a, b, c, d)	SG: Molting CE: Secondary cement production I	Protein heterodimerization
A0A131XKB4 Puromycin-sensitive aminopeptidase (a, c)	SG: Cement maintenance CE: Detachment	Proteolysis
Q45R50 Salivary gland metalloprotease (a, c)	SG: Molting CE: Cement maintenance	Proteolysis
A0A131YLU7/A0A224Y1G3* Aminopeptidase N (b, c, d)	CE: Feeding SG: Detachment	Proteolysis
A0A224Z8F0 Transglutaminase/protease like protein (b, c, d)	CE: Detachment	Proteolysis
A0A131ZAV6 Reprolysin (c)	CE: Detachment	Proteolysis
A0A224YTI7 Angiotensin-converting enzyme (c, d)	CE: Secondary cement production I	Proteolysis
A0A224YD77 Gluzincin (c)	CE: Cement maintenance	Proteolysis
A0A131YF72 Glycine-rich superfamily member (b, c)	CE: Detachment	Putative cell wall structural and/or cuticle protein
A0A034WWS7 Secreted cement protein 2 (b, c)	CE: Molting	Putative cell wall structural and/or cuticle protein
L7MDN1 Putative glycine rich protein	CE: Molting	Putative cell wall structural and/or cuticle protein 63% identity (E=6.8e-40) to *Amblyomma*

(b, c)		*parvum* Putative nuclear pore proteinucleoporin 62 (A0A023G321)
A0A224YCP1 Glycine-rich superfamily member (b, c)	CE: Cement maintenance	Putative cell wall structural and/or cuticle protein
A0A224YEB4 Glycine-rich superfamily member (b, c)	CE: Secondary cement production II	Putative cell wall structural and/or cuticle protein
A0A034WZ79 Glycine-rich protein 3 (b, c)	CE: Secondary cement production II	Putative cell wall structural and/or cuticle protein
L7M1K6 Putative glycine rich protein (b, c)	CE: Feeding	Putative cell wall structural and/or cuticle protein
A0A224YEQ4¶* Glycine rich superfamily member (a, b, c)	SG: Molting CE: Cement maintenance	Putative cell wall structural and/or cuticle protein 76% identity (E=0.0) to *Tabanus bromius* Putative alpha-1 collagen type iii (A0A0K8TMJ9)
A0A224Y271 Pancreatic trypsin inhibitor (c)	CE: Molting	Negative regulation of endopeptidase activity
A0A131YNG2 Pancreatic trypsin inhibitor (c)	CE: Cement maintenance	Negative regulation of endopeptidase activity
A0A224Y1X4 Pancreatic trypsin inhibitor (c)	CE: Cement maintenance	Negative regulation of endopeptidase activity
L7LRL1 Putative bilaris (c)	CE: Molting	Negative regulation of endopeptidase activity
L7ME64 Putative bilaris (c)	CE: Cement maintenance	Negative regulation of endopeptidase activity
A0A224YMC8 Lipocalin (c)	CE: Molting	Evasion or tolerance of host defense response
A0A224YB96 Lipocalin (c)	CE: Secondary cement production II	Evasion or tolerance of host defense response
L7LTA8 Putative group II salivary lipocalin (c)	CE: Secondary cement production II	Evasion or tolerance of host defense response
G3MKF8 Tubulin beta chain (a)	SG: Feeding & oogenesis CE: Feeding & oogenesis	Cytoskeleton organization & microtubule-based process
A0A034WXM6 Secreted protein 20 (a)	SG: Feeding & oogenesis CE: Detachment	Unknown 43% identity (E= 4.8e-55) to *Odontobuthus doriae* (Yellow Iranian scorpion) Venom

		protein VP6 (A0A0U3YCW0)
A0A034WXN6 Hemelipoprotein HeLp 2 (a)	SG: Cement maintenance CE: Cement maintenance	Lipid transport
A0A034WZ42 Hemelipoprotein HeLp (a)	SG: Secondary cement production I CE: Cement maintenance	Lipid transport
A0A224YTB6 Alpha-N-acetylgalactosaminidase (a)	SG: Secondary cement production I CE: Secondary cement production II	Carbohydrate metabolic process
L7M046 Cuticular protein (a)	SG: Molting CE: Secondary cement production II	Chitin metabolic process
A0A0K8RP30 Putative ubiquitin/40s ribosomal protein s27a fusion (b)	CE: Feeding and oogenesis	Unknown
A0A0B4PMF7 Peptidoglycan recognition protein (d)	CE: Cement maintenance	Peptidoglycan catabolic process
A0A131YG55 Peptidoglycan recognition protein (d)	CE: Cement maintenance	Peptidoglycan catabolic process
B7Q181 Cytochrome P450 (d)	CE: Cement maintenance	Metabolic process
L7M9R2 Putative animal peptidoglycan recognition protein logous to bacteriophage t3 lysozyme (d)	CE: Secondary cement production II	Innate immune response Peptidoglycan catabolic process

Tick cementome proteins were first selected based on one of the following criteria: (a) identified in both sialome and cementome, (b) being among the two proteins with highest representation in feeding, feeding and oogenesis, molting, secondary cement production, cement maintenance or detachment categories, and predicted to play a key role in tick-host interactions due to (c) over 4% representation in biological processes (Figure 4B) or (d) after network analysis. ¶These proteins appeared also as one of the two proteins with highest representation in secondary cement production (Q4PM69 and A0A224YU86) or cement maintenance (A0A224YEQ4). *Proteins selected for validation correspond to those fulfilling 3 to 4 of the selection criteria a-d. Abbreviations: SG, salivary gland; CE, cement.

Table S2. Cattle host-derived proteins identified in *R. microplus* tick cementome.

Protein ID and name	Representation profile category	Biological Process
P00921 Carbonic anhydrase 2	SG: Feeding & oogenesis CE: Feeding & oogenesis	Angiotensin-activated signaling pathway Positive regulation of dipeptide transmembrane transport Regulation of anion transport Regulation of intracellular Ph
F1MSZ6 Antithrombin-III	SG: Feeding & oogenesis CE: Feeding & oogenesis	Negative regulation of endopeptidase activity Regulation of blood coagulation, intrinsic pathway
P34955 Alpha-1-antiproteinase	SG: Feeding & oogenesis CE: Feeding & oogenesis	Negative regulation of endopeptidase activity
P63243 Receptor of activated protein C kinase 1	SG: Secondary cement production CE: Feeding & oogenesis	Cell cycle Cellular response to glucose stimulus Cellular response to growth factor stimulus Gastrulation Negative regulation of cell growth Negative regulation of gene expression Negative regulation of hydrogen peroxide-induced neuron death Negative regulation of peptidyl-serine phosphorylation Negative regulation of phagocytosis Negative regulation of protein kinase B signaling Negative regulation of Wnt signaling pathway Pigmentation Positive regulation of apoptotic process Positive regulation of cell migration Positive regulation of cyclic-nucleotide phosphodiesterase activity Positive regulation of gastrulation Positive regulation of Golgi to plasma membrane protein transport Positive regulation of GTPase activity Positive regulation of intrinsic apoptotic signaling pathway Positive regulation of mitochondrial depolarization Positive regulation of proteasomal ubiquitin-dependent protein catabolic process Positive regulation of protein homooligomerization Positive regulation of protein phosphorylation Protein ubiquitination Regulation of cell cycle

		Regulation of cell división Regulation of establishment of cell polarity Regulation of protein localization Rescue of stalled ribosome Rhythmic process
Q1JPB0 Leukocyte elastase inhibitor	SG: Feeding CE: Feeding & oogenesis	Negative regulation of endopeptidase activity
Q2KJF1 Alpha-1B-glycoprotein Immunoglobulin supergene family	SG: Feeding & oogenesis CE: Feeding & oogenesis	Neutrophil degranulation Platelet degranulation
Q8SPJ1 Junction plakoglobin	SG: Secondary cement production CE: Feeding & oogenesis	Bundle of His cell-Purkinje myocyte adhesion involved in cell communication Cell migration Cellular response to indole-3-methanol Desmosome assembly Detection of mechanical stimulus Endothelial cell-cell adhesión Negative regulation of blood vessel endothelial cell migration Positive regulation of angiogénesis Positive regulation of cell-matrix adhesión Positive regulation of DNA-binding transcription factor activity Positive regulation of protein import into nucleus Positive regulation of transcription by RNA polymerase II Protein localization to plasma membrane Regulation of cell population proliferation Regulation of heart rate by cardiac conduction Regulation of ventricular cardiac muscle cell action potential Skin development
Q9BGI3Peroxiredoxin-2	SG: Feeding & oogenesis CE: Feeding & oogenesis	Activation of MAPK activity Cell redox homeostasis Homeostasis of number of cells Hydrogen peroxide catabolic process Leukocyte activation Negative regulation of extrinsic apoptotic signaling pathway in absence of ligand Negative regulation of lipopolysaccharide-mediated signaling pathway Negative regulation of NF-kappaB transcription factor activity Negative regulation of reactive oxygen species metabolic process Negative regulation of T cell differentiation Positive regulation of blood coagulation Regulation of hydrogen peroxide metabolic process Removal of superoxide radicals Respiratory burst involved in inflammatory

		response Response to lipopolysaccharide Response to oxidative stress T cell proliferation Thymus development
A0A0F6QNP7 Complement component 3	SG: Feeding & oogenesis CE: Feeding & oogenesis	Complement activation Inflammatory response
G5E604Uncharacterized protein	SG: Feeding & oogenesis CE: Feeding & oogenesis	Immune response Immunoglobulin production
B0JYN6* Alpha-2-HS-glycoprotein	SG: Feeding & oogenesis CE: Feeding & oogenesis	Acute-phase response Negative regulation of bone mineralization Ossification Positive regulation of phagocytosis Regulation of inflammatory response
B5T254 Peptidoglycan-recognition protein	SG: Secondary cement production CE: Feeding & oogenesis	Innate immune response Peptidoglycan catabolic process
D4QBB4 Globin A1	SG: Feeding & oogenesis CE: Feeding & oogenesis	Oxygen transport
E1B6Z6Lipocalin 2	SG: Feeding & oogenesis CE: Feeding & oogenesis	Defense response to bacterium Extrinsic apoptotic signaling pathway in absence of ligand Innate immune response Positive regulation of cold-induced thermogenesis Response to virus Sequestering of iron ion Siderophore transport
E1BKT9* Desmoplakin	SG: Secondary cement production CE: Feeding & oogenesis	Adherens junction organization Bundle of His cell-Purkinje myocyte adhesion involved in cell communication Cell-cell adhesion Desmosome organization Intermediate filament cytoskeleton organization Intermediate filament organization Keratinocyte differentiation Peptide cross-linking Protein localization to adherens junction Regulation of heart rate by cardiac conduction Regulation of ventricular cardiac muscle cell action potential Skin development Ventricular compact myocardium morphogenesis

		Wound healing
F1N076Ceruloplasmin	SG: Feeding & oogenesis CE: Feeding & oogenesis	Cellular iron ion homeostasis Copper ion transport Iron ion homeostasis Iron ion transport
G3N0V2¶*Keratin 1	SG: Secondary cement production CE: Feeding & oogenesis	Complement activation, lectin pathway Establishment of skin barrier Negative regulation of inflammatory response Peptide cross-linking Protein heterotetramerization
G5E513Uncharacterized protein	SG: Feeding & oogenesis CE: Feeding & oogenesis	B cell receptor signaling pathway Complement activation, classical pathway Defense response to bacterium Innate immune response Phagocytosis, engulfment Phagocytosis, recognition Positive regulation of B cell activation
G8JKW7 Uncharacterized protein	SG: Feeding & oogenesis CE: Feeding & oogenesis	Negative regulation of endopeptidase activity
Q5EA67 Inter-alpha (Globulin) inhibitor H4 (Plasma Kallikrein-sensitive glycoprotein)	SG: Feeding & oogenesis CE: Feeding & oogenesis	Hyaluronan metabolic process
Q5J801 Endopin 2B	SG: Feeding & oogenesis CE: Feeding & oogenesis	Neural regulation
V6F9A2 Apolipoprotein A-I preproprotein	SG: Feeding & oogenesis CE: Feeding & oogenesis	Adrenal gland development Blood vessel endothelial cell migration Cholesterol biosynthetic process Cholesterol efflux Cholesterol homeostasis Cholesterol import Endothelial cell proliferation Glucocorticoid metabolic process G protein-coupled receptor signaling pathway High-density lipoprotein particle assembly High-density lipoprotein particle remodeling Integrin-mediated signaling pathway Lipid storage Lipoprotein biosynthetic process Lipoprotein metabolic process Negative regulation of cell adhesion molecule production Negative regulation of cytokine secretion

		involved in immune response Negative regulation of heterotypic cell-cell adhesion Negative regulation of hydrolase activity Negative regulation of inflammatory response Negative regulation of interleukin-1 beta secretion Negative regulation of tumor necrosis factor-mediated signaling pathway Negative regulation of very-low-density lipoprotein particle remodeling Peptidyl-methionine modification Phosphatidylcholine biosynthetic process Phospholipid efflux Phospholipid homeostasis Positive regulation of cholesterol efflux Positive regulation of cholesterol esterification Positive regulation of hydrolase activity Positive regulation of lipid biosynthetic process Positive regulation of phagocytosis Positive regulation of phospholipid efflux Positive regulation of Rho protein signal transduction Positive regulation of stress fiber assembly Positive regulation of substrate adhesion-dependent cell spreading Protein oxidation Protein stabilization Regulation of Cdc42 protein signal transduction Regulation of cholesterol transport Regulation of intestinal cholesterol absorption Regulation of protein phosphorylation Reverse cholesterol transport Triglyceride catabolic process Triglyceride homeostasis Very-low-density lipoprotein particle remodeling Vitamin transport
F1MN78 Serpin B4	SG: Secondary cement production CE: Feeding & oogenesis	Negative regulation of peptidase activity Protection from natural killer cell mediated cytotoxicity Regulation of proteolysis
A0A1K0FUD3Globin C1	SG: Feeding & oogenesis CE: Feeding & oogenesis	Oxygen transport Transport
F1MC11¶* Keratin, type I cytoskeletal 14	SG: Secondary cement production CE: Feeding & oogenesis	Aging Epithelial cell differentiation Hair cycle Intermediate filament bundle assembly
Q7SIH1 Alpha-2-macroglobulin	SG: Feeding & oogenesis	Blood coagulation, intrinsic pathway Extracellular matrix disassembly

	CE: Feeding & oogenesis	Negative regulation of complement activation, lectin pathway Platelet degranulation Regulation of small GTPase mediated signal transduction Stem cell differentiation
M0QVY0Uncharacterized protein	SG: Secondary cement production CE: Feeding & oogenesis	Unknown
Q1RMN8Immunoglobulin light chain, lambda gene cluster	SG: Secondary cement production CE: Feeding & oogenesis	B cell receptor signaling pathway Complement activation, classical pathway Defense response to bacterium Innate immune response Leukocyte migration Phagocytosis, recognition and engulfment Positive regulation of B cell activation
G5E5H7Uncharacterized protein	SG: Secondary cement production CE: Feeding	Unknown
A6QNZ7*Keratin 10 (Epidermolytic hyperkeratosis; keratosis palmaris et plantaris)	SG: Secondary cement production CE: Feeding	Keratinocyte differentiation Peptide cross-linking Protein heterotetramerization
P02662Alpha-S1-casein	SG: Secondary cement production CE: Detachment	Negative regulation of apoptotic process Negative regulation of gene expression Negative regulation of supramolecular fiber organization Positive regulation of androst-4-ene-3,17-dione biosynthetic process Positive regulation of androstenedione secretion Positive regulation of progesterone biosynthetic process Positive regulation of progesterone secretion Protein stabilization Response to 11-deoxycorticosterone Response to dehydroepiandrosterone Response to estradiol Response to growth hormone Response to progesterone
P02663Alpha-S2-casein	SG: Secondary cement production CE: Detachment	Defense response to bacterium Response to 11-deoxycorticosterone Response to dehydroepiandrosterone Response to estradiol Response to growth hormone Response to progesterone
Q0P5J4*Keratin, type I cytoskeletal 25	SG: Secondary cement production CE: Detachment	Aging Cytoskeleton organization Hair follicle morphogenesis Intermediate filament organization

Q08D91* Keratin, type II cytoskeletal 75	SG: Secondary cement production CE: Detachment	Hematopoietic progenitor cell differentiation Protein polymerization
Q148H5* Keratin, type II cytoskeletal 71	SG: Feeding CE: Detachment	Hair follicle morphogenesis Intermediate filament organization Protein polymerization
A0A140T897 Serum albumin	SG: Feeding & oogenesis CE: Detachment	Cellular response to starvation Maintenance of mitochondrion location Negative regulation of apoptotic process Negative regulation of protein oligomerization
A5PJE3Fibrinogen alpha chain	SG: Feeding & oogenesis CE: Detachment	Platelet activation Protein polymerization
D4QBB3 Hemoglobin beta	SG: Feeding & oogenesis CE: Detachment	Oxygen transport Transport
G3MZ71* Keratin 2	SG: Secondary cement production CE: Detachment	Intermediate filament organization Keratinization Keratinocyte activation Keratinocyte development Keratinocyte migration Keratinocyte proliferation Peptide cross-linking Positive regulation of epidermis development
Q3SZZ9FGG protein	SG: Feeding & oogenesis CE: Detachment	Platelet activation Protein polymerization
Q9TTE1Serpin A3-1	SG: Feeding & oogenesis CE: Secondary cement production	Negative regulation of endopeptidase activity
G3N0V0 Uncharacterized protein	SG: Feeding & oogenesis CE: Secondary cement production	B cell receptor signaling pathway Complement activation, classical pathway Defense response to bacterium Innate immune response Phagocytosis, engulfment Phagocytosis, recognition Positive regulation of B cell activation
Q3SZV7Hemopexin	SG: Secondary cement production CE: Secondary cement production	Cellular iron ion homeostasis Heme metabolic process Hemoglobin metabolic process Positive regulation of humoral immune response mediated by circulating immunoglobulin Positive regulation of immunoglobulin production Positive regulation of interferon-gamma-mediated signaling pathway Positive regulation of tyrosine phosphorylation of STAT protein

G5E5T5Uncharacterized protein	SG: Feeding CE: Secondary cement production	Unknown
G3X6N3Serotransferrin	SG: Feeding & oogenesis CE: Secondary cement production	Cellular iron ion homeostasis Cellular response to iron ion Positive regulation of receptor-mediated endocytosis Regulation of iron ion transport
F1MAV0 Fibrinogen beta chain	SG: Feeding & oogenesis CE: Secondary cement production	Platelet activation Protein polymerization
G3MXL3* Keratin 3	SG: Secondary cement production CE: Secondary cement production	Cornification Epithelial cell differentiation Intermediate filament cytoskeleton organization Keratinization
A4FUZ0* Keratin, type II cuticular Hb3	SG: Feeding CE: Secondary cement production	Aging Cornification Epidermis development Keratinization
Q148I8* Keratin 31	SG: Secondary cement production CE: Secondary cement production	Cornification Epidermis development Keratinization

Cattle host-derived proteins identified in *R. microplus* tick cementome were selected based on the identification in both sialome and cementome. Abbreviations: SG, salivary gland; CE, cement. ¶Proteins represented with more than 1 million TAS at all time points. *Proteins selected for validation correspond to those putatively involved in cement formation, solidification and maintenance.

Table S3. Comparative analysis of amino acid composition of cattle host and tick *R. microplus* derived proteins identified in the cementome.

Parameter	**Host**	**Tick**	**Host cement**	**Tick cement**
Theoretical pI	4.75	4.88	4.76	5.73
Amino acid composition				
Ala (A)	9.2%	8.7%	12.5%	6.8%
Arg (R)	4.2%	4.0%	3.1%	4.8%
Asn (N)	4.0%	4.2%	5.1%	3.0%
Asp (D)	5.8%	6.0%	5.2%	4.2%
Cys (C)	1.6%	1.8%	1.8%	2.0%
Gln (Q)	4.6%	3.8%	5.9%	2.7%
Glu (E)	7.5%	7.1%	8.8%	4.7%
Gly (G)	10.2%	8.4%	3.9%	15.5%
His (H)	1.5%	2.3%	1.9%	1.8%
Ile (I)	5.3%	4.6%	4.6%	3.9%
Leu (L)	9.6%	10.5%	8.9%	10.2%
Lys (K)	4.2%	4.4%	5.3%	2.6%
Met (M)	0.7%	0.6%	0.7%	0.6%
Phe (F)	3.6%	4.5%	5.5%	4.8%
Pro (P)	6.3%	5.6%	5.7%	6.3%
Ser (S)	6.4%	6.6%	6.3%	8.0%
Thr (T)	5.4%	5.2%	3.0%	4.3%
Trp (W)	0.5%	0.9%	1.0%	0.8%
Tyr (Y)	2.6%	3.1%	3.8%	6.4%
Val (V)	7.0%	7.9%	7.1%	6.6%
Pyl (O)	0.0%	0.0%	0.0%	0.0%
Sec (U)	0.0%	0.0%	0.0%	0.0%
Asn or Asx (B)	n = 10.0%	n = 0.0%	n = 0.0%	n = 0.0%
Gln or Glu (Z)	n = 0.0%	n = 0.0%	n = 0.0%	n = 0.0%
Unknown (X)	n = 0.0%	n = 0.0%	n = 0.0%	n = 0.0%
Percent of negatively charged residues (D + E)	13.3%	13.2%	14.0%	8.9%
Percent of positively charged residues (R + K)	8.4%	8.4%	8.4%	7.4%
Ratio of negatively to positively charged residues	1.6	1.6	1.7	1.2
Atomic composition*	Unknown			
Carbon C		31.9%	32.2%	32.5%
Hydrogen H		49.6%	49.4%	49.2%
Nitrogen N		8.5%	8.4%	8.6%
Oxygen O		9.8%	9.8%	9.6%
Sulfur S		0.2%	0.2%	0.2%
Instability index**	37.91 Stable	37.47 Stable	37.30 Stable	36.74 Stable
Aliphatic index**	87.31	90.29	85.60	81.02
Grand average of hydropathicity (GRAVY)**	-0.220	-0.147	-0.245	-0.073

Data for all cattle host-derived proteins identified in the cementome but not in the sialome (Host), 100 randomly selected tick-derived proteins identified in the sialome but not in the cementome (Tick), all host-derived proteins identified in the sialome and cementome (Host cement), and all tick-derived proteins identified in the cementome (Tick cement) (Data S7) were analyzed using the ProtParam tool (https://web.expasy.org/protparam/).

*When at least one ambiguous position (B, Z or X) is found in the sequence considered, the atomic composition cannot be computed.

**Calculated for the sum of all peptide sequences.

Table S4. Recombinant tick proteins used for validation by Western blot analysis.

Protein name and ID	DNA and RT-PCR primer sequences	Protein sequence
Q4PM69 Histone H4	>Complete cds atgtctggccgtggcaaaggtggcaaggggctc ggaaaaggaggcgccaagcgtcatcgcaaggtg ctccgagacaacatccaggggatcacaaagccc gccattcgtcgtctggctcgccgtggtggcgtc aagcgtatctccggtctgatctacgaggagacc cgaggcgtgctcaaagtcttcctggagaacgtg atccgcgacgccgtcacctacacggaacacgcc aagagaaaaacggtcaccgccatggacgtcgtc tacgcgctgaagagacaaggacgtaccctgtac gggttcggcggctag	MSGRGKGGKGLGK GGAKRHRKVLRDN IQGITKPAIRRLA RRGGVKRISGLIY EETRGVLKVFLEN VIRDAVTYTEHAK RKTVTAMDVVYAL KRQGRTLYGFGG
Q4PM69 Histone H4	>Primer sequences: 5′ – 3′ Forward (F) and Reverse (R) F: CTCGAGATGTCTGGCCGTGGCAAAG R: GAATTCGCCGCCGAACCCGTACAGGG	
A0A131YLU7 Aminopeptidase N	>Peptidase M domain atggtggattattcgttatcaattggtccaaag atcttggaattctacgagaagtacttctcggaa aagtatccactcccaaagactgacatggtggca ctgccggactttaatgctggcgccatggagaat tggggactggtcaccttccgagaaacggctcta ctcttcaacccgaacgagtcgtcggccggaaac aagcagcgcgtcgccgtcgtcgtctcacatgaa ctcgcacatcagtggtttggaaacttagttacc atggagtggtgggacgacctgtggctcaatgaa ggcttcgccacctacgttgagtatctgggcgtg gatttcgttcacaaggactgggagatggcacaa cagttcatcggcgaagaactgcagccagtgatg gagctcgactccctcaagtcgtcgcaccctgtc tcggttccagtctacaaccctgacgaaatcatt gaaaactttgacaagatatcttacggaaagggg gcatccataattcgtatgatgaacttcttcctc acagaaccggtcttcaggaaaggtgtctcgact tacctgaagaaacgctctttcaacaacgctcgc caggatgatctttgggcggaactcaccatggct caaaatgaaagcaaccgcgtggacgtcaagact gtgatggattcgtggactctc	MVDYSLSIGPKIL EFYEKYFSEKYPL PKTDMVALPDFNA GAMENWGLVTFRE TALLFNPNESSAG NKQRVAVVVSHEL AHQWFGNLVTMEW WDDLWLNEGFATY VEYLGVDFVHKDW EMAQQFIGEELQP VMELDSLKSSHPV SVPVYNPDEIIEN FDKISYGKGASII RMMNFFLTEPVFR KGVSTYLKKRSFN NARQDDLWAELTM AQNESNRVDVKTV MDSWTL
A0A131YLU7 Aminopeptidase N	>Primer sequences: 5′ – 3′ Forward (F) and Reverse (R) F: CTCGAGATGGTGGATTATTCGTTA R: GAATTCGAGAGTCCACGAATCCAT	
A0A224YEQ4 Glycine-rich superfamily member	>Optimized sequence atgtatccgggtagcttcggtggcgtgctgggt cgtctgagcggcagctatccgggtagcctgggt ggcgttctgggtggcctgtacggcagctatccg ggtcgtttcggtggcgcgctgagcggtctgtat ggcagctatccgggtagctttggtggctacctg ggtggcctgagcggttacatgtatccgggcagc tttggtggcgtgctgggccgtctgagcggtagc tatccgggcagcctgggtggcgttctgggtggc ctgtatggtagctatccgggccgtttcggtggc gcgctgtctggcttatatggcagctatccgggt	MYPGSFGGVLGRL SGSYPGSLGGVLG GLYGSYPGRFGGA LSGLYGSYPGSFG GYLGGLSGYMYPG SFGGVLGRLSGSY PGSLGGVLGGLYG SYPGRFGGALSGL YGSYPGSFGGYLG GLSGYMYPGSFGG VLGRLSGSYPGSL

	agctttggtggctacctgggtggcctgtctggc tatatgtatccgggcagcttcggtggcgtgtta ggtcgtctgtctggcagctatccgggtagcctg ggtggcgttctgggtggcctgtacggcagctat ccgggtcgtttcggtggcgcgctgagtggcctt tatggcagctatccgggtagctttggtggctac ctgggtggcctgagtggctacatgtatccgggc agctttggtggcgtgttaggccgtctgtctggt agctatccgggcagcctgggtggcgttctgggt ggcctgtacggtagctatccgggccgtttcggt ggcgcgctgagtgggttgtatggcagctatccg ggtagctttggtggctacctgggtggcctgagt gggtacatgtatccgggcagcttcggtggcgtg cttggtcgtctgtccggcagctatccgggtagc ctgggtggcgttctgggtggcctgtacggcagc tatccgggtcgtttcggtggcgcgctgagtggt ttatatggcagctatccgggtagctttggtggc tacctgggtggcctgagtggttatatgtatccg ggcagctttggtggcgtgctaggccgtctgagt ggtagctatccgggtagcctgggtggtgtgctg ggtggcctgtacggtagctatccgggccgtttc ggtggcgcgctgagtggactctatggcagctat ccgggtagctttggtggctacctgggtggcctg agtggatacatgtatccgggtagcttcggtggc gtgttaggtcgtctgagtggcagctatccgggt agcctgggtggtgtgctgggtggcctgtacggc agctatccgggtcgtttcggtggcgcgctgagt gggctatatggcagctatccgggtagctttggt ggctacctgggtggcctgagtgggtacatgtat ccgggtagctttggtggcgtgttgggccgtctg tctggtagctatccgggtagcctgggtggtgtg ctgggtggcctgtacggtagctatccgggccgt ttcggtggcgcgctgagtgggctgtatggcagc tatccgggtagctttggtggctacctgggtggc ctgagtgggtacatgtatccgggtagcttcggt ggcgtgctaggtcgtctgagcggcagctatccg ggtagcctgggtggtgtgctgggtggcctgtac ggcagctatccgggtcgtttcggtggcgcgctg agtgggctttatggcagctatccgggtagcttt ggtggctacctgggtggcctgagtgggtacatg tatccgggtagcttcggtggcgtgctcggccgt ctgtccggtagctatccgggtagcctgggtggt gtgctgggtggcctgtacggtagctatccgggc cgtttcggtggcgcgctgagtgggctctatggc agctatccgggtagctttggtggctacctgggt ggcctgagtgggtac	GGVLGGLYGSYPG RFGGALSGLYGSY PGSFGGYLGGLSG YMYPGSFGGVLGR LSGSYPGSLGGVL GGLYGSYPGRFGG ALSGLYGSYPGSF GGYLGGLSGYMYP GSFGGVLGRLSGS YPGSLGGVLGGLY GSYPGRFGGALSG LYGSYPGSFGGYL GGLSGYMYPGSFG GVLGRLSGSYPGS LGGVLGGLYGSYP GRFGGALSGLYGS YPGSFGGYLGGLS GYMYPGSFGGVLG RLSGSYPGSLGGV LGGLYGSYPGRFG GALSGLYGSYPGS FGGYLGGLSGYMY PGSFGGVLGRLSG SYPGSLGGVLGGL YGSYPGRFGGALS GLYGSYPGSFGGY LGGLSGYMYPGSF GGVLGRLSGSYPG SLGGVLGGLYGSY PGRFGGALSGLYG SYPGSFGGYLGGL SGYMYPGSFGGVL GRLSGSYPGSLGG VLGGLYGSYPGRF GGALSGLYGSYPG SFGGYLGGLSGY
A0A224YEQ4 Glycine-rich superfamily member	>Primer sequences: 5′ – 3′ Forward (F) and Reverse (R) F: CACCATGTATCCGGGTAGCTTCGG R: CCCACTCAGGCCACCCAGGT	

Table S5. Examples of tick-derived proteins identified in this study in the cementome and previously characterized and reported in the sialome/sialotranscriptome.

Protein names	**References**
Secreted protein 20 Hemelipoprotein HeLp/ HeLp 2	Tirloni L, Reck J, Terra RM, Martins JR, Mulenga A, Sherman NE, Fox JW, Yates JR 3rd, Termignoni C, Pinto AF, Vaz Ida S Jr. Proteomic Analysis of Cattle Tick *Rhipicephalus* (*Boophilus*) *microplus* Saliva: A Comparison between Partially and Fully Engorged Females. PLoS One. 2014 Apr 24;9(4):e94831.
Puromycin-sensitive aminopeptidase	Ribeiro JM, Slovák M, Francischetti IM. An insight into the sialome of *Hyalomma excavatum.* Ticks Tick Borne Dis. 2017 Feb;8(2):201-207. Ayllón N, Villar M, Galindo RC, Kocan KM, Šíma R, López JA, Vázquez J, Alberdi P, Cabezas-Cruz A, Kopáček P, de la Fuente J. Systems biology of tissue-specific response to *Anaplasma phagocytophilum* reveals differentiated apoptosis in the tick vector *Ixodes scapularis*. PLoS Genet. 2015 Mar 27;11(3):e1005120.
Tubulin beta chain	Karim S, Singh P, Ribeiro JM. A Deep Insight into the Sialotranscriptome of the Gulf Coast Tick, *Amblyomma maculatum.* PLoS One. 2011;6(12):e28525.
Myosin heavy chain 6/7 Glycine-rich superfamily member Alpha-N-acetylgalactosaminidase Transglutaminase/protease like protein	de Castro MH, de Klerk D, Pienaar R, Rees DJG, Mans BJ. Sialotranscriptomics of *Rhipicephalus zambeziensis* reveals intricate expression profiles of secretory proteins and suggests tight temporal transcriptional regulation during blood-feeding. Parasit Vectors. 2017 Aug 10;10(1):384. Ayllón N, Villar M, Galindo RC, Kocan KM, Šíma R, López JA, Vázquez J, Alberdi P, Cabezas-Cruz A, Kopáček P, de la Fuente J. Systems biology of tissue-specific response to *Anaplasma phagocytophilum* reveals differentiated apoptosis in the tick vector *Ixodes scapularis*. PLoS Genet. 2015 Mar 27;11(3):e1005120.
Cuticular protein	Tan AW, Francischetti IM, Slovak M, Kini RM, Ribeiro JM. Sexual differences in the sialomes of the zebra tick, *Rhipicephalus pulchellus.* J Proteomics. 2015 Mar 18;117:120-44. Ayllón N, Villar M, Galindo RC, Kocan KM, Šíma R, López JA, Vázquez J, Alberdi P, Cabezas-Cruz A, Kopáček P, de la Fuente J. Systems biology of tissue-specific response to *Anaplasma phagocytophilum* reveals differentiated apoptosis in the tick vector *Ixodes scapularis*. PLoS Genet. 2015 Mar 27;11(3):e1005120.
Aminopeptidase N	de Castro MH, de Klerk D, Pienaar R, Latif AA, Rees DJ, Mans BJ. De novo assembly and annotation of the salivary gland transcriptome of *Rhipicephalus appendiculatus* male and female ticks during blood feeding. Ticks Tick Borne Dis. 2016 Jun;7(4):536-48. Ayllón N, Villar M, Galindo RC, Kocan KM, Šíma R, López JA, Vázquez J, Alberdi P, Cabezas-Cruz A, Kopáček P, de la Fuente J. Systems biology of tissue-specific response to *Anaplasma phagocytophilum* reveals differentiated apoptosis in the tick vector *Ixodes scapularis*. PLoS Genet. 2015 Mar 27;11(3):e1005120.

Aminopeptidase Glycine-rich superfamily member Myosin	Lewis LA, Radulović ŽM, Kim TK, Porter LM, Mulenga A. Identification of 24 h *Ixodes scapularis* immunogenic tick saliva proteins. Ticks Tick Borne Dis. 2015 Apr;6(3):424-34. de Castro MH, de Klerk D, Pienaar R, Latif AA, Rees DJ, Mans BJ. De novo assembly and annotation of the salivary gland transcriptome of *Rhipicephalus appendiculatus* male and female ticks during blood feeding. Ticks Tick Borne Dis. 2016 Jun;7(4):536-48. Esteves E, Maruyama SR, Kawahara R, Fujita A, Martins LA, Righi AA, Costa FB, Palmisano G, Labruna MB, Sá-Nunes A, Ribeiro JMC, Fogaça AC. Analysis of the Salivary Gland Transcriptome of Unfed and Partially Fed *Amblyomma sculptum* Ticks and Descriptive Proteome of the Saliva. Front Cell Infect Microbiol. 2017 Nov 21;7:476. Ayllón N, Villar M, Galindo RC, Kocan KM, Šíma R, López JA, Vázquez J, Alberdi P, Cabezas-Cruz A, Kopáček P, de la Fuente J. Systems biology of tissue-specific response to *Anaplasma phagocytophilum* reveals differentiated apoptosis in the tick vector *Ixodes scapularis*. PLoS Genet. 2015 Mar 27;11(3):e1005120. Bullard R, Sharma SR, Das PK, Morgan SE, Karim S. Repurposing of Glycine-rich proteins in abiotic and biotic stresses in the Lone-Star tick (*Amblyomma americanum*). Front Physiol. 2019 Jun 18;10:744. Kim TK, Tirloni L, Pinto AFM, Diedrich JK, Moresco JJ, Yates JR 3rd, da Silva Vaz I Jr, Mulenga A. Time-resolved proteomic profile of *Amblyomma americanum* tick saliva during feeding. PLoS Negl Trop Dis. 2020;14(2):e0007758.
Salivary gland metalloprotease Reprolysin	Barnard AC, Nijhof AM, Gaspar AR, Neitz AW, Jongejan F, Maritz-Olivier C. Expression profiling, gene silencing and transcriptional networking of metzincin metalloproteases in the cattle tick, *Rhipicephalus (Boophilus) microplus*. Vet Parasitol. 2012 May 25;186(3-4):403-14. Anatriello E, Ribeiro JM, de Miranda-Santos IK, Brandão LG, Anderson JM, Valenzuela JG, Maruyama SR, Silva JS, Ferreira BR. An insight into the sialotranscriptome of the brown dog tick, *Rhipicephalus sanguineus*. BMC Genomics. 2010 Jul 22;11:450. Ayllón N, Villar M, Galindo RC, Kocan KM, Šíma R, López JA, Vázquez J, Alberdi P, Cabezas-Cruz A, Kopáček P, de la Fuente J. Systems biology of tissue-specific response to *Anaplasma phagocytophilum* reveals differentiated apoptosis in the tick vector *Ixodes scapularis*. PLoS Genet. 2015 Mar 27;11(3):e1005120.
Lipocalin	Tirloni L, Kim TK, Pinto AFM, Yates JR 3rd, da Silva Vaz

	I Jr, Mulenga A. Tick-Host Range Adaptation: Changes in Protein Profiles in Unfed Adult *Ixodes scapularis* and *Amblyomma americanum* Saliva Stimulated to Feed on Different Hosts. Front Cell Infect Microbiol. 2017 Dec 19;7:517. Esteves E, Maruyama SR, Kawahara R, Fujita A, Martins LA, Righi AA, Costa FB, Palmisano G, Labruna MB, Sá-Nunes A, Ribeiro JMC, Fogaça AC. Analysis of the Salivary Gland Transcriptome of Unfed and Partially Fed *Amblyomma sculptum* Ticks and Descriptive Proteome of the Saliva. Front Cell Infect Microbiol. 2017 Nov 21;7:476. Manzano-Román R, Díaz-Martín V, Oleaga A, Obolo-Mvoulouga P, Pérez-Sánchez R. TSGP4 from *Ornithodoros moubata*: molecular cloning, phylogenetic analysis and vaccine efficacy of a new member of the lipocalin clade of cysteinyl leukotriene scavengers. Vet Parasitol. 2016 Aug 30;227:130-7. Neelakanta G, Sultana H, Sonenshine DE, Andersen JF. Identification and characterization of a histamine-binding lipocalin-like molecule from the relapsing fever tick *Ornithodoros turicata*. Insect Mol Biol. 2018 Apr;27(2):177-187. de Castro MH, de Klerk D, Pienaar R, Latif AA, Rees DJ, Mans BJ. De novo assembly and annotation of the salivary gland transcriptome of *Rhipicephalus appendiculatus* male and female ticks during blood feeding. Ticks Tick Borne Dis. 2016 Jun;7(4):536-48. Anatriello E, Ribeiro JM, de Miranda-Santos IK, Brandão LG, Anderson JM, Valenzuela JG, Maruyama SR, Silva JS, Ferreira BR. An insight into the sialotranscriptome of the brown dog tick, *Rhipicephalus sanguineus*. BMC Genomics. 2010 Jul 22;11:450. Francischetti IM, My Pham V, Mans BJ, Andersen JF, Mather TN, Lane RS, Ribeiro JM. The transcriptome of the salivary glands of the female western black-legged tick *Ixodes pacificus* (Acari: Ixodidae). Insect Biochem Mol Biol. 2005 Oct;35(10):1142-61. Ayllón N, Villar M, Galindo RC, Kocan KM, Šíma R, López JA, Vázquez J, Alberdi P, Cabezas-Cruz A, Kopáček P, de la Fuente J. Systems biology of tissue-specific response to *Anaplasma phagocytophilum* reveals differentiated apoptosis in the tick vector *Ixodes scapularis*. PLoS Genet. 2015 Mar 27;11(3):e1005120. Kim TK, Tirloni L, Pinto AFM, Diedrich JK, Moresco JJ, Yates JR 3rd, da Silva Vaz I Jr, Mulenga A. Time-resolved proteomic profile of *Amblyomma americanum* tick saliva during feeding. PLoS Negl Trop Dis. 2020;14(2):e0007758.
Pancreatic trypsin inhibitor	Tirloni L, Kim TK, Coutinho ML, Ali A, Seixas A, Termignoni C, Mulenga A, da Silva Vaz I Jr. The putative role of *Rhipicephalus microplus* salivary serpins in the tick-

	host relationship. Insect Biochem Mol Biol. 2016 Apr;71:12-28. Zhang H, Qiao R, Gong H, Cao J, Zhou Y, Zhou J. Identification and anticoagulant activity of a novel Kunitz-type protein HA11 from the salivary gland of the tick *Hyalomma asiaticum*. Exp Appl Acarol. 2017 Jan;71(1):71-85.
Peptidoglycan recognition protein	Wang J, Song X, Wang M. Peptidoglycan recognition proteins in hematophagous arthropods. Dev Comp Immunol. 2018 Jun;83:89-95. Shaw DK, Wang X, Brown LJ, Chávez AS, Reif KE, Smith AA, Scott AJ, McClure EE, Boradia VM, Hammond HL, Sundberg EJ, Snyder GA, Liu L, DePonte K, Villar M, Ueti MW, de la Fuente J, Ernst RK, Pal U, Fikrig E, Pedra JH. Infection-derived lipids elicit an immune deficiency circuit in arthropods. Nat Commun. 2017 Feb 14;8:14401.
Cytochrome P450	Rosario-Cruz R, Almazan C, Miller RJ, Dominguez-Garcia DI, Hernandez-Ortiz R, de la Fuente J. Genetic basis and impact of tick acaricide resistance. Front Biosci (Landmark Ed). 2009 Jan 1;14:2657-65. Ayllón N, Villar M, Galindo RC, Kocan KM, Šíma R, López JA, Vázquez J, Alberdi P, Cabezas-Cruz A, Kopáček P, de la Fuente J. Systems biology of tissue-specific response to *Anaplasma phagocytophilum* reveals differentiated apoptosis in the tick vector *Ixodes scapularis*. PLoS Genet. 2015 Mar 27;11(3):e1005120.
Angiotensin-converting enzyme	Jarmey JM, Riding GA, Pearson RD, McKenna RV, Willadsen P. Carboxydipeptidase from *Boophilus microplus*: a "concealed" antigen with similarity to angiotensin-converting enzyme. Insect Biochem Mol Biol. 1995 Oct;25(9):969-74. Riding GA, Jarmey J, McKenna RV, Pearson R, Cobon GS, Willadsen P. A protective "concealed" antigen from *Boophilus microplus*. Purification, localization, and possible function. J Immunol. 1994 Dec 1;153(11):5158-66.

Table S6. Published results about the potential role of selected tick cementome proteins for novel vaccine development.

Protein name and ID	Results	Reference
Secreted protein 20 A0A034WXM6	Potential vaccine antigen for the control of tick paralysis caused by *Ixodes holocyclus*	Masina et al., 1999
Myosin heavy chain 6/7 A0A224YU86	Protective response against tick, *Haemaphysalis qinghaiensis*	Gao et al., 2007
Salivary gland metalloprotease Reprolysin Q45R50 A0A131ZAV6	Protective response against ticks, *Ixodes ricinus*, *Haemaphysalis longicornis* and *R. microplus*	Decrem et al., 2008 Imamura et al., 2009 Ali et al., 2015
Alpha-N-acetylgalactosaminidase A0A224YTB6	Characterization as a potential vaccine antigen in *Clonorchis sinensis* (human clonorchiasis)	Lee et al., 2012
Cuticular protein L7M046	Protective response against *Haemonchus contortus* (human and animal haemonchosis) and *Wuchereria bancrofti* (human lymphatic filariasis)	Boisvenue et al., 1991 Arunkumar et al., 2014
Aminopeptidase N A0A131YLU7	Protective response as a mosquito-based vaccine against malaria	Mathias et al., 2012
Transglutaminase/protease like protein A0A224Z8F0	Protective response against human lymphatic filariasis	Immanuel et al., 2017
Lipocalins A0A224YMC8 A0A224YB96 L7LTA8	Protective response against tick, *Ixodes ricinus* and *A. phagocytophilum* infection	Contreras et al., 2017
Angiotensin-converting enzyme A0A224YTI7	Protective response against tick, *R. microplus*	Willadsen et al., 1996 Lambertz et al., 2012
Tubulin beta chain G3MKF8	Protective response against *Trypanosoma evansi* challenge	Tewari et al., 2015

Data refers to selected tick cementome proteins identified in this study (Table S1). Results have not been reported for histones H2A, H3, H4 (V5HZA1, V5HJX3, L7LVH9, Q4PM69), hemelipoproteins HeLp and HeLp 2 (A0A034WXN6, A0A034WZ42), Glycine-rich superfamily members (A0A224YEQ4, A0A224YEB4, A0A034WZ79, L7MDN1, A0A224YCP1, L7M1K6, A0A131YF72, A0A034WWS7), putative ubiquitin/40s ribosomal protein s27a fusion (A0A0K8RP30), puromycin-sensitive aminopeptidase (A0A131XKB4), pancreatic trypsin inhibitors (A0A224Y271, A0A131YNG2, A0A224Y1X4), putative bilaris (L7LRL1, L7ME64), gluzincin (A0A224YD77), peptidoglycan recognition proteins (A0A0B4PMF7, A0A131YG55), Cytochrome P450 (B7Q181), and putative animal peptidoglycan recognition protein logous to bacteriophage t3 lysozyme (L7M9R2).

References included in Table S6

Ali A, Parizi LF, Guizzo MG, Tirloni L, Seixas A, Vaz Ida S Jr, Termignoni C. Immunoprotective potential of a *Rhipicephalus (Boophilus) microplus* metalloprotease. Vet Parasitol. 2015 Jan 15;207(1-2):107-14. doi: 10.1016/j.vetpar.2014.11.007

Arunkumar C, Pandiaraja P, Prince PR, Kaliraj P. Immunological characterization of recombinant *Wuchereria bancrofti* cuticular collagen (COL-4) as putative vaccine candidate for human lymphatic filariasis. Asian Pac J Trop Med. 2014 Jul;7(7):505-12. doi: 10.1016/S1995-7645(14)60084-5

Boisvenue RJ, Stiff MI, Tonkinson LV, Cox GN. Protective studies in sheep immunized with cuticular collagen proteins and peptides of *Haemonchus contortus*. Parasite Immunol. 1991 May;13(3):227-40.

Contreras, M., Alberdi, P., Fernández de Mera, I.G., Krull, C., Nijhof, A., Villar, M., de la Fuente, J. 2017. Vaccinomics approach to the identification of candidate protective antigens for the control of tick vector infestations and *Anaplasma phagocytophilum* infection. Frontiers in Cellular and Infection Microbiology 7: 360.

Decrem Y, Mariller M, Lahaye K, Blasioli V, Beaufays J, Zouaoui Boudjeltia K, Vanhaeverbeek M, Cérutti M, Brossard M, Vanhamme L, Godfroid E. The impact of gene knock-down and vaccination against salivary metalloproteases on blood feeding and egg laying by *Ixodes ricinus*. Int J Parasitol. 2008 Apr;38(5):549-60.

Gao J, Luo J, Fan R, Guan G, Ren Q, Ma M, Sugimoto C, Bai Q, Yin H. Molecular characterization of a myosin alkali light chain-like protein, a "concealed" antigen from the hard tick *Haemaphysalis qinghaiensis*. Vet Parasitol. 2007 Jun 20;147(1-2):140-9.

Imamura S, da Silva Vaz I Jr, Konnai S, Yamada S, Nakajima C, Onuma M, Ohashi K. Effect of vaccination with a recombinant metalloprotease from *Haemaphysalis longicornis*. Exp Appl Acarol. 2009 Aug;48(4):345-58. doi: 10.1007/s10493-009-9245-3

Immanuel C, Ramanathan A, Balasubramaniyan M, Khatri VK, Amdare NP, Rao DN, Reddy MVR, Perumal K. Immunoprophylaxis of multi-antigen peptide (MAP) vaccine for human lymphatic filariasis. Immunol Res. 2017 Jun;65(3):729-738. doi: 10.1007/s12026-017-8911-5

Lambertz C, Chongkasikit N, Jittapalapong S, Gauly M. Immune Response of Bos indicus Cattle against the Anti-Tick Antigen Bm91 Derived from Local *Rhipicephalus (Boophilus) microplus* Ticks and Its Effect on Tick Reproduction under Natural Infestation. J Parasitol Res. 2012;2012:907607. doi: 10.1155/2012/907607

Lee MR, Yoo WG, Kim YJ, Kim DW, Cho SH, Hwang KY, Ju JW, Lee WJ. Molecular characterization of an α-N-acetylgalactosaminidase from *Clonorchis sinensis*. Parasitol Res. 2012 Nov;111(5):2149-56. doi: 10.1007/s00436-012-3063-y. Erratum in: Parasitol Res. 2012 Dec;111(6):2483.

Masina S, Broady KW. Tick paralysis: development of a vaccine. Int J Parasitol. 1999 Apr;29(4):535-41.

Mathias DK, Plieskatt JL, Armistead JS, Bethony JM, Abdul-Majid KB, McMillan A, Angov E, Aryee MJ, Zhan B, Gillespie P, Keegan B, Jariwala AR, Rezende W, Bottazzi ME, Scorpio DG, Hotez PJ, Dinglasan RR. Expression, Immunogenicity, Histopathology, and Potency of a Mosquito-Based Malaria Transmission-Blocking Recombinant Vaccine. Infect Immun. 2012 Apr;80(4):1606-14. doi: 10.1128/IAI.06212-11

Tewari AK, Kurup SP, Baidya S, Barta JR, Sharma B. Protective antibody and cytokine responses in mice following immunization with recombinant beta-tubulin and subsequent *Trypanosoma evansi* challenge. Parasit Vectors. 2015 Nov 9;8:580. doi: 10.1186/s13071-015-1189-3

Willadsen P, Smith D, Cobon G, McKenna RV. Comparative vaccination of cattle against *Boophilus microplus* with recombinant antigen Bm86 alone or in combination with recombinant Bm91. Parasite Immunol. 1996 May;18(5):241-6.

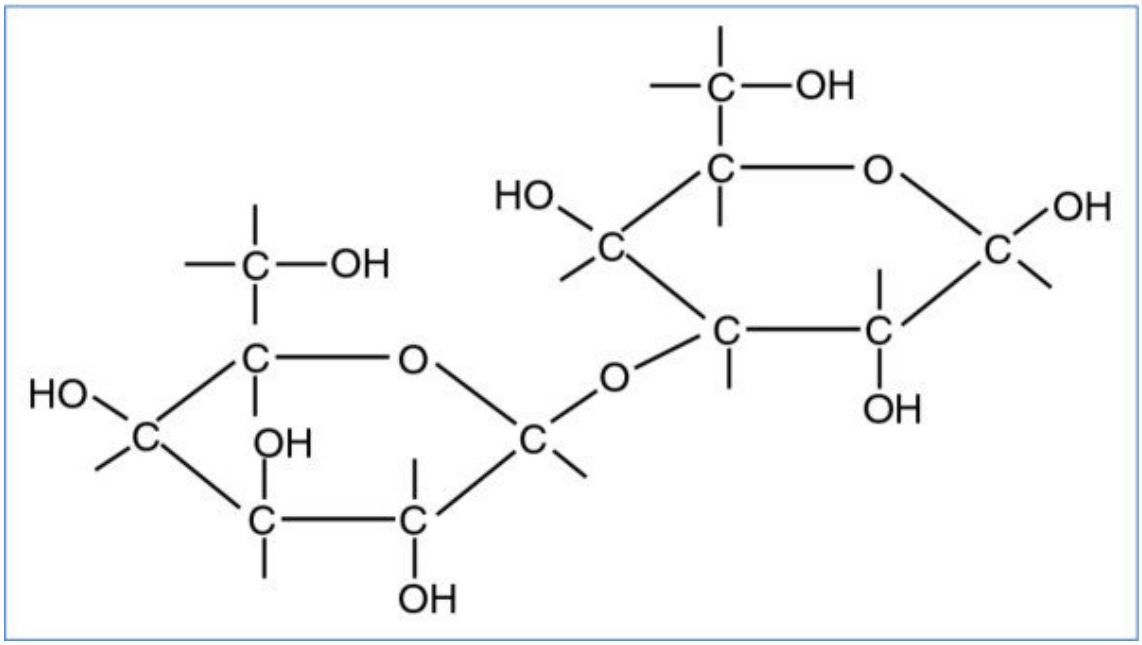

Atomic composition	
Carbon C	38.7%
Oxygen O	35.5%
Hydrogen H	25.8%

Figure S1. Chemical structure and atomic composition of Galα1-3Galβ1-(3)4GlcNAc-R (α-Gal; $C_{12}H_8O_{11}$).

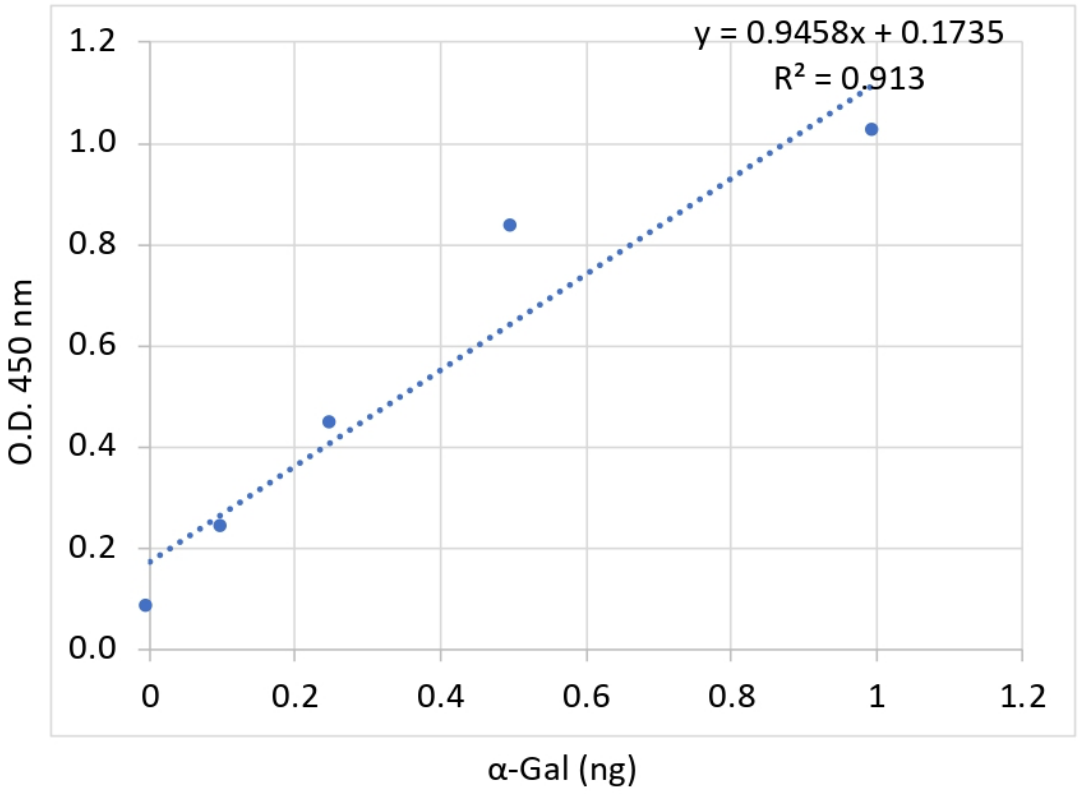

Figure S2. ELISA test for characterizing α-Gal levels. The α-Gal levels were determined by ELISA using BSA-α-Gal and *R. microplus* sialome and cementome proteins. The average value of the blanks (wells without sample proteins; N = 5) was subtracted from all reads and the average of 9 replicates for each sample was used for analysis. A calibration curve with 0.0 to 1.0 ng α-Gal and O.D. values at 450 nm was constructed using Microsoft Excel for Mac (v. 16.26) to convert ELISA reader values to α-Gal content per sample.

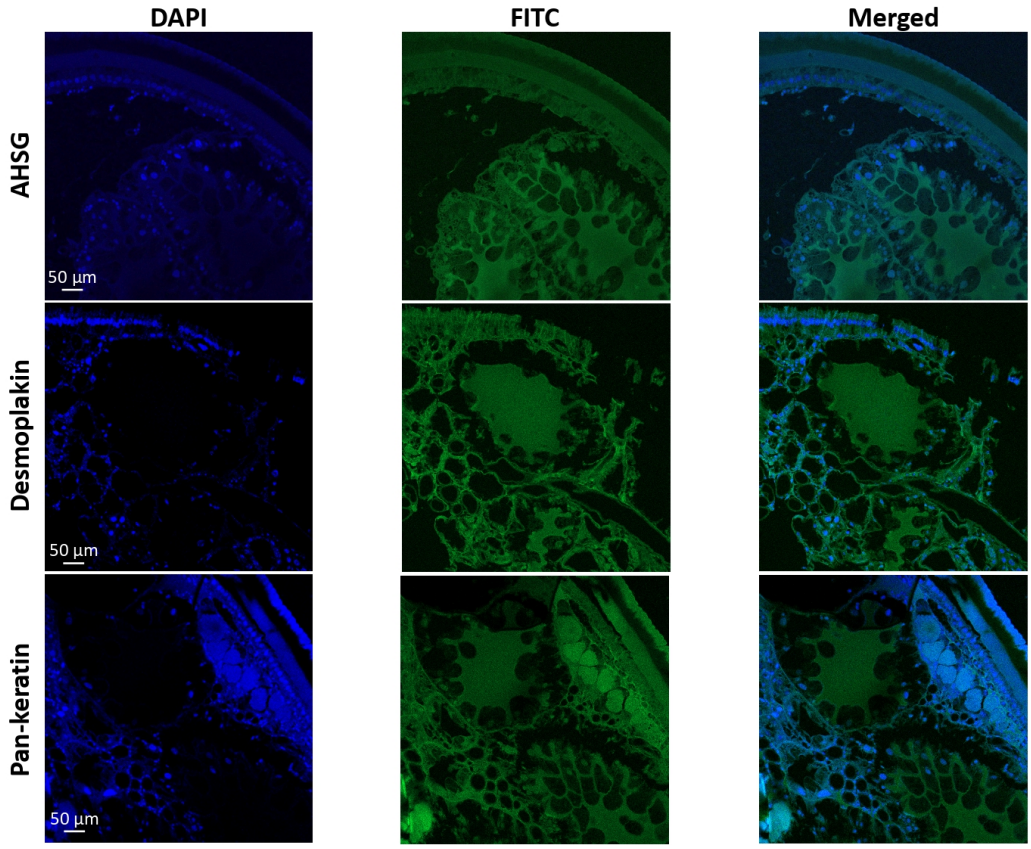

Figure S3. Validation of commercial antibodies against host proteins by immunofluorescence assay. Female *Ixodes scapularis* ticks fed on uninfected sheep and fixed with 4% paraformaldehyde in 0.2 M sodium cacodylate buffer were embedded in paraffin and used to prepare sections on glass slides as previously described (Ayllón et al., PLoS Genetics 2015;11: e1005120 and de la Fuente et al., Computational and Structural Biotechnology Journal 2020;18: 253-257). The paraffin was removed from the sections with xylene and then hydrated by successive 2 min washes with a graded series of 100, 95, 80, 75, and 50% ethanol. The slides were treated with Proteinase K (Dako, Barcelona, Spain) for 7 min, washed with PBS and incubated with 3% BSA (Sigma-Aldrich) in PBS for 1 h at RT. Then the slides were incubated with antibodies against desmoplakin (ab106342) and pan-keratin (ab190625) (Abcam, Cambridge, UK) diluted 1:100 in 3% BSA/PBS for 14 h at 4 °C. After additional washes in PBS, the sections were incubated with FITC conjugated goat anti-rabbit IgG secondary antibodies (Sigma-Aldrich), diluted 1:80 in 3% BSA/PBS, for 1 h at RT. Finally, the slides were mounted using Prolong Gold antifade reagent with DAPI reagent (Molecular Probes, Eugene, OR, USA). The slides were examined using a Zeiss LSM 800 laser scanning confocal microscope (Carl Zeiss, Oberkochen, Germany) with a 10x objective.

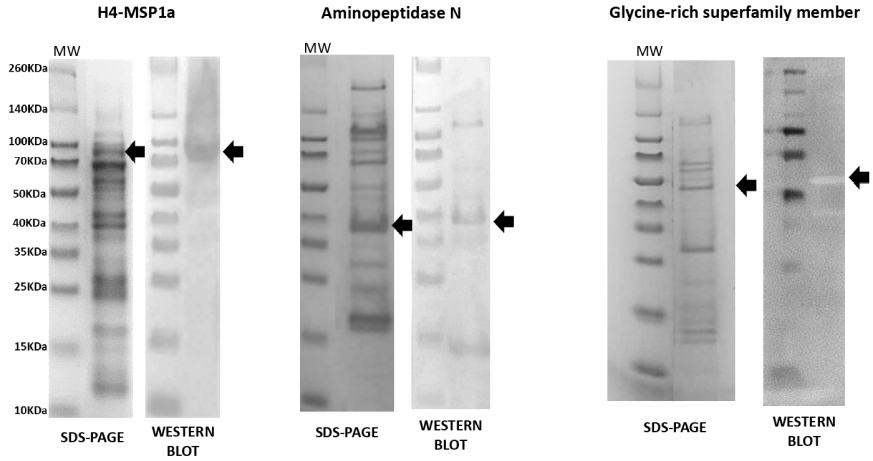

Figure S4. Western blot analysis of recombinant tick proteins. The recombinant histone H4-MSP1a, aminopeptidase N, and Glycine-rich superfamily member proteins were produced in *E. coli*. Samples were taken after purification. Ten µg proteins were loaded per well in an SDS-12% polyacrylamide gel. The gel was stained with Coomassie Brilliant Blue. The position of the recombinant proteins is indicated with arrows. For Western blot analysis, recombinant proteins were separated by electrophoresis and transferred to a nitrocellulose membrane. The membrane was incubated with pooled sera collected from histone H4, aminopeptidase N vaccinated rabbits and commercial rabbit anti-Glycine-rich superfamily member protein antibodies (Abcam). The position of the recombinant proteins in the Western blot is indicated with arrows. Abbreviation: MW, molecular weight markers (Spectra multicolor broad range protein ladder; Thermo Fisher Scientific).

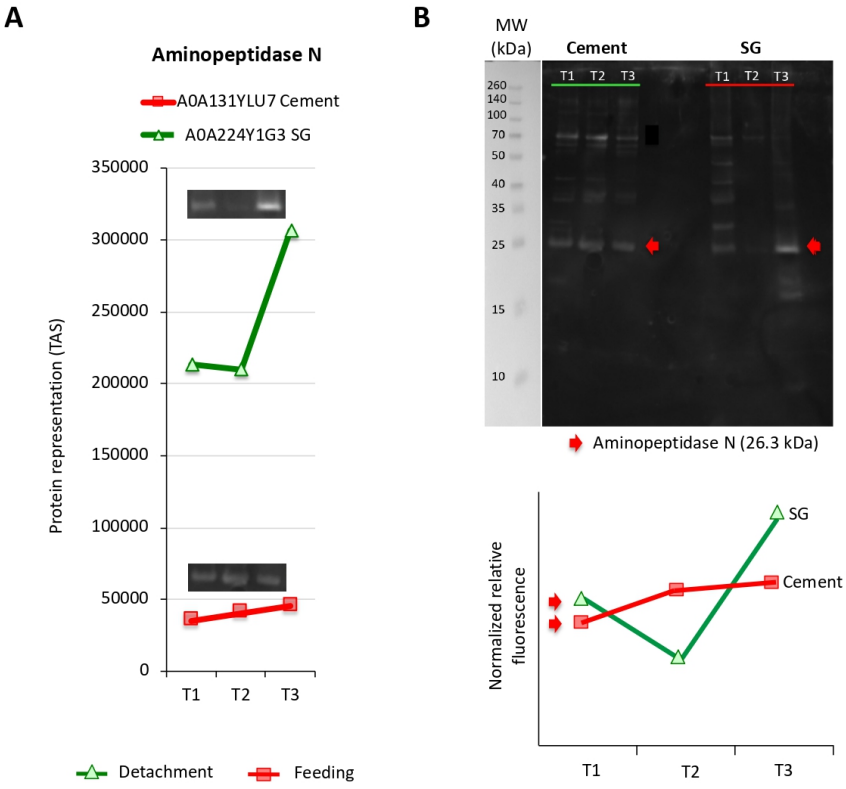

Figure S5. Western blot analysis of tick-derived aminopeptidase N protein in the *R. microplus* cementome (Cement) and sialome (SG). (A) Based on proteomics representation profiles, proteins were putatively assigned to different categories of developmental processes (Figure 1). (B) Cement protein lysate (10 µg) and salivary gland protein lysate (20 µg) were methanol/chloroform precipitated, resuspended in Laemmli sample buffer and separated on an SDS-polyacrylamide precast gel (ClearPage Expedeon, VWR, Radnor, PA, USA). After electrophoresis, proteins were transferred to a nitrocellulose blotting membrane (GE Healthcare Dharmacon Inc., Lafayette, CO, USA), blocked with 3% BSA (Sigma-Aldrich) in TBS and incubated overnight at 4 °C with antibodies against tick recombinant aminopeptidase N, diluted 1:200 in 3% BSA/TBS. To detect the IgG antibodies bound to tick proteins, membranes were incubated with goat anti-rabbit IgG peroxidase antibody (Sigma-Aldrich) diluted 1:1000 in 3% BSA/TBS. Immunoreactive proteins were visualized with chemiluminescence with Pierce ECL Western Blotting Substrate (Thermo Fisher Scientific). Quantitative analysis was performed using the Fiji ImageJ (https://imagej.nih.gov/ij/download.html) to measure the intensity of the protein bands and after substation of the intensity of the PBS control to compare the results at different time points. The results of the Western blot reproduced those obtained with proteomics analysis.

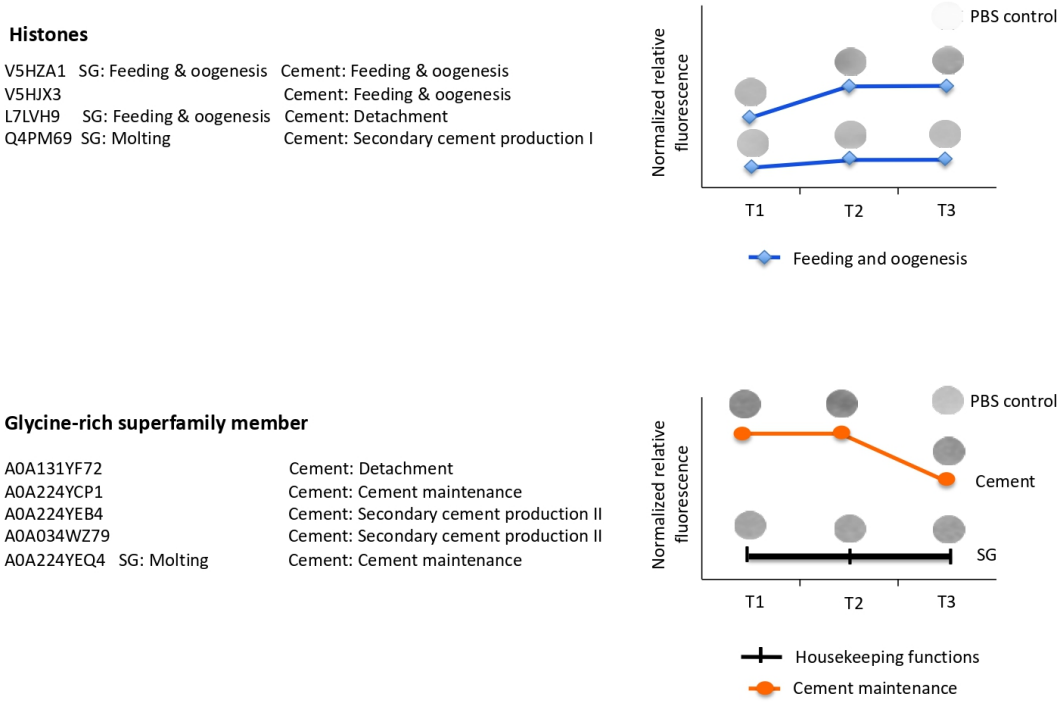

Figure S6. Dot blot analysis of tick-derived histones and Glycine-rich superfamily member proteins in the *R. microplus* cementome (Cement) and sialome (SG). Cement and salivary gland proteins were applied onto each strip in 6 different dots (volume per dot, 25 µl at 5 µg/µl. Then the dots were allowed to dry by gravity flow, immersed in 50 µl of 3% BSA/TBS for 15 min approximately and filtered by gravity. Membranes were washed two times with TBS and incubated with primary antibodies diluted at different concentrations in 1% BSA/TBS against Histone H4 (1:100) and Glycine-rich superfamily member proteins (1:200) To detect the IgG antibodies bound to tick proteins, membranes were incubated with goat anti-rabbit IgG peroxidase antibody (Sigma-Aldrich) diluted 1:1000 in 1% BSA/TBS. Membranes were washed two times with TBS and immunoreactive proteins were visualized with chemiluminescence with Pierce ECL Western Blotting Substrate (Thermo Fisher Scientific). Quantitative analysis was performed using the Fiji ImageJ (https://imagej.nih.gov/ij/download.html) to measure the intensity of the protein bands and after substation of the intensity of the PBS control to compare the results at different time points. Based on proteomics representation profiles, proteins were putatively assigned to different categories of developmental processes (Figure 1). Because these proteins constitute a protein family they were assigned to multiple developmental processes. Accordingly, the results of the dot blot reproduced some of the profiles obtained with proteomics analysis.

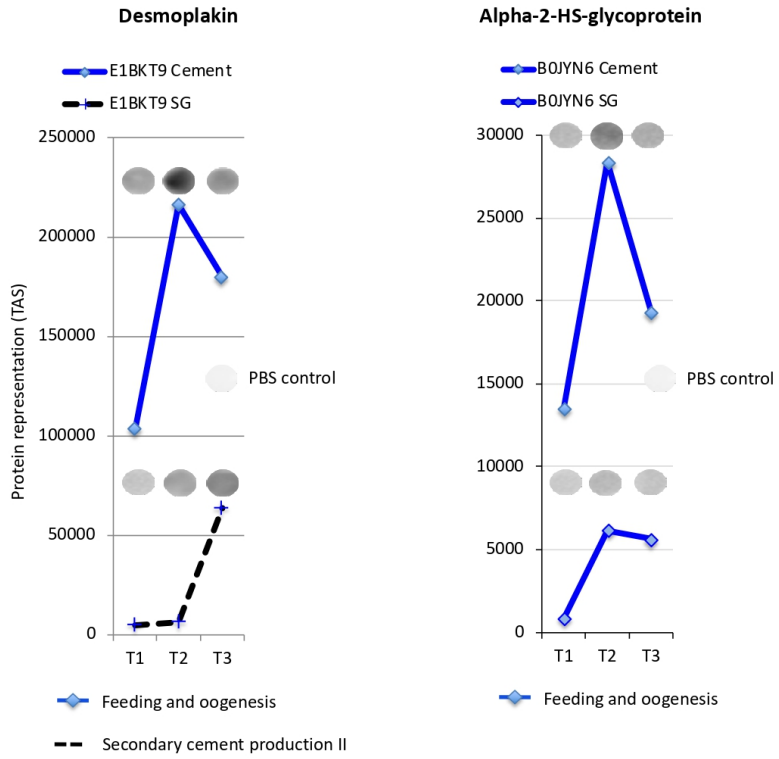

Figure S7. Dot blot analysis of host-derived desmoplakin and alpha-2-HS-glycoprotein in the *R. microplus* cementome (Cement) and sialome (SG). Cement and salivary gland proteins were applied onto each strip in 6 different dots (volume per dot, 25 µl at 5 µg/µl. Then the dots were allowed to dry by gravity flow, immersed in 50 µl of 3% BSA/TBS for 15 min approximately and filtered by gravity. Membranes were washed two times with TBS and incubated with primary antibodies diluted at different concentrations in 1% BSA/TBS against desmoplakin (1:300) and alpha-2-HS-glycoprotein (1:300). To detect the IgG antibodies bound to tick proteins, membranes were incubated with goat anti-rabbit IgG peroxidase antibody (Sigma-Aldrich) diluted 1:1000 in 1% BSA/TBS. Membranes were washed two times with TBS and immunoreactive proteins were visualized with chemiluminescence with Pierce ECL Western Blotting Substrate (Thermo Fisher Scientific). Quantitative analysis was performed using the Fiji ImageJ (https://imagej.nih.gov/ij/download.html) to measure the intensity of the protein bands and after substation of the intensity of the PBS control to compare the results at different time points. Based on proteomics representation profiles, proteins were putatively assigned to different categories of developmental processes (Figure 1). Because these proteins constitute a protein family they were assigned to multiple developmental processes. The results of the dot blot reproduced those obtained with proteomics analysis.

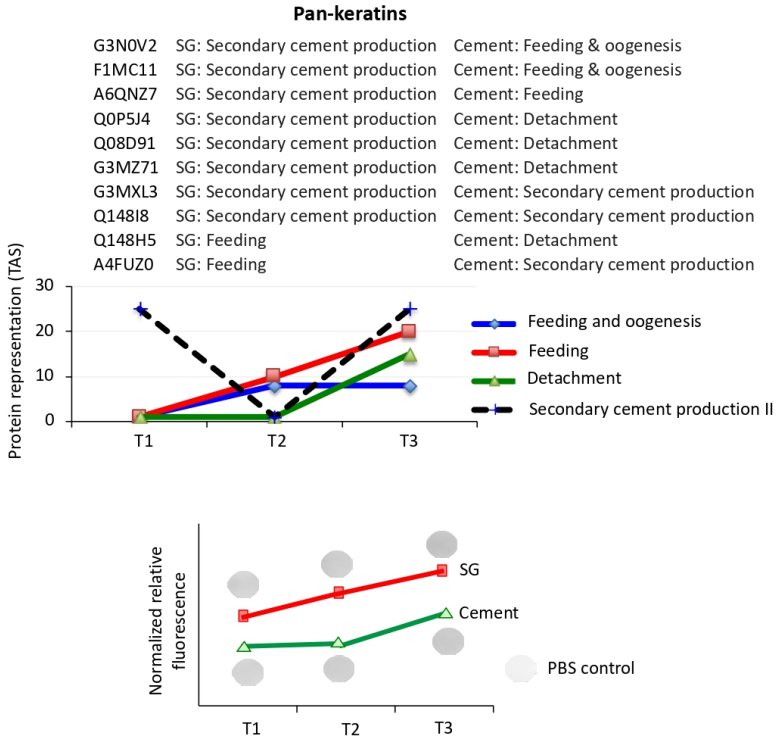

Figure S8. Dot blot analysis of host-derived pan-keratins in the *R. microplus* cementome (Cement) and sialome (SG). Cement and salivary gland proteins were applied onto each strip in 6 different dots (volume per dot, 25 µl at 5 µg/µl. Then the dots were allowed to dry by gravity flow, immersed in 50 µl of 3% BSA/TBS for 15 min approximately and filtered by gravity. Membranes were washed two times with TBS and incubated with primary antibodies diluted 1:300 in 1% BSA/TBS against pan-keratins. To detect the IgG antibodies bound to tick proteins, membranes were incubated with goat anti-rabbit IgG peroxidase antibody (Sigma-Aldrich) diluted 1:1000 in 1% BSA/TBS. Membranes were washed two times with TBS and immunoreactive proteins were visualized with chemiluminescence with Pierce ECL Western Blotting Substrate (Thermo Fisher Scientific). Quantitative analysis was performed using the Fiji ImageJ (https://imagej.nih.gov/ij/download.html) to measure the intensity of the protein bands and after substation of the intensity of the PBS control to compare the results at different time points. Based on proteomics representation profiles, proteins were putatively assigned to different categories of developmental processes (Figure 1). Because these proteins constitute a protein family they were assigned to multiple developmental processes. Accordingly, the results of the dot blot reproduced some of the profiles obtained with proteomics analysis.